JOURNAL OF AIRCRAFT
Vol. 41, No. 6, November–December 2004

# Model for Parachute Canopy Deformation and Feedback on Descent Properties

Mayer Humi*
*Worcester Polytechnic Institute, Worcester, Massachusatts 01609-2280*

**A complete treatment of parachute large deformations and descent, after deployment, requires the solution of the fluid-structure interaction problem and the consideration of many other dynamical issues such as wake reattachment. Furthermore, because of the transient nature of the problem it is not easy to simulate the obtain physical insights about the dynamical behavior of the system. To achieve some of these insights, we present in this paper a low-dimensional model for circular parachute, which captures the essence of this problem. This model is coupled then with a flow simulation program (which is based on the vortex method) to gauge the impact of the fluid-structure interaction on the dynamics of this system.**

## Nomenclature

| | | |
|---|---|---|
| $A_h$ | = | projected horizontal area of the circular canopy |
| $A_v$ | = | projected vertical area of the circular canopy |
| $C_D$ | = | drag coefficient of the system |
| $C_L$ | = | coefficient of lift |
| $E$ | = | Young modulus of the rod |
| $\boldsymbol{e}$ | = | unit vector in the direction of the tension in the cords |
| $\boldsymbol{F}(l)$ | = | resultant stress on a cross section of the rod at $l$ |
| $g$ | = | acceleration of gravity, 9.8 m/s$^2$ |
| $h$ | = | length of the elastic cord(s) under loading |
| $h_0$ | = | natural length of the elastic cords |
| $I$ | = | moment of inertia of the rod |
| $k$ | = | elastic constant of the cords |
| $L$ | = | length of the rod |
| $l$ | = | distance of a point on the rod from its center |
| $M(l)$ | = | moment acting on the rod at $l$ |
| $M_{\text{fs}}$ | = | pitching moment caused by fluid-structure interaction |
| $m$ | = | $m_0 + \rho_A V(t)$ |
| $m_c$ | = | mass of the cargo |
| $m_0$ | = | mass of the parachute-cargo system |
| $\boldsymbol{n}$ | = | normal to the rod at each point |
| $p$ | = | fluid pressure |
| $\boldsymbol{r}$ | = | position of a point on the rod, $= (x, y)$ |
| $\boldsymbol{T}$ | = | tension in elastic cords connecting the rod to the cargo |
| $t$ | = | time |
| $\boldsymbol{t}(l)$ | = | tangent to the rod at $l$ |
| $\boldsymbol{u}$ | = | fluid velocity, $= (u, v)$ |
| $\boldsymbol{u}_p$ | = | parachute velocity, $= (u_p, v_p)$, $u_p^2 = \boldsymbol{u}_p \cdot \boldsymbol{u}_p$ |
| $V(t)$ | = | volume in the circular canopy, which is generated by rotation of the rod around the axis vertical to its tangent at the center |
| $\boldsymbol{v}_c$ | = | cargo velocity |
| $\boldsymbol{x}_c$ | = | cargo position |
| $\Gamma_i$ | = | circulation of the $i$th vortex |
| $\nu$ | = | fluid viscosity |
| $\rho$ | = | linear density of rod |
| $\rho_A$ | = | air density |
| $\psi$ | = | angle between the horizontal ($x$ axis) and the tangent to the rod at its center (pitching angle) |
| $\omega$ | = | vorticity |

Received 4 April 2003; revision received 27 February 2004; accepted for publication 19 March 2004. 

*Professor, Department of Mathematical Sciences, 100 Institute Road; mhumi@wpi.edu.

## I. Introduction

NUMERICAL simulations of fully deployed circular parachutes advanced considerably in the last two decades because of increase in computational power and new algorithms.[1–3] However in spite of these advances, the full treatment of the fluid-structure interaction for this problem remains largely as an open problem, which continues to be investigated experimentally.[4,5] Furthermore it is not easy to obtain from the numerical simulations or experimental data deep insights about the dynamical aspects of the parachute-cargo system during descent and possible bifurcations in its behavior that might lead to its failure. This is caused in part by the wide range of parameters that control this dynamics and its transient nature.

In the past attempts for semi-analytic treatments of this problem (which blend experimental data and some simulations) under some major simplifications were presented by Ross[6–8] and Piscitelle.[9] In particular Ross[6] presented a model for flat circular parachute in steady vertical descent. Under these assumptions the canopy has a constant shape, and problems related to parachute deformation and oscillations are not present. The simulation work of the Sandia group on parachute inflation and descent incorporated some approximate representation of the elastic properties of the canopy and suspension lines.[10–12] Also there have been several earlier papers dedicated to the simulation of canopy oscillations using off-diagonal apparent mass matrix terms in the equations of motion.[12–21] However, in spite of these investigations we believe that there exists at present no transparent semi-analytic treatment which takes into consideration the impact that large deformations and oscillations have on parachute dynamics.

It is our objective in this paper to present a preliminary model with small numbers of degrees of freedom, which are capable of addressing these issues. To derive this model, we assume that the canopy can be represented by an inextendable elastic bar whose shape corresponds to a cross section of the canopy. The rest of system consists of the cargo and two massless elastic cords, which connect the cargo to the canopy (see Fig. 1). We neglect torsion.

The representation of the canopy by an inextendable elastic bar has been used in Refs. 1, 2, 6, and 22 and is not new. It allows us to reduce the system to one in two dimensions and study its behavior under this approximation. In this regard the model presented here can be considered as preliminary to a more realistic one in three dimensions, where the canopy is represented by a collection of such elastic rods in three-dimensional configuration and the cargo attached to each of these rods by massless elastic cords. It should be observed also that the materials used today to construct the canopy satisfy to a good approximation the assumption of inextendability under "normal" loads.

The modeling process is carried out in three stages. In the first stage we consider only the static state of the system. Next we consider the system subject to deformations, oscillations, and vertical

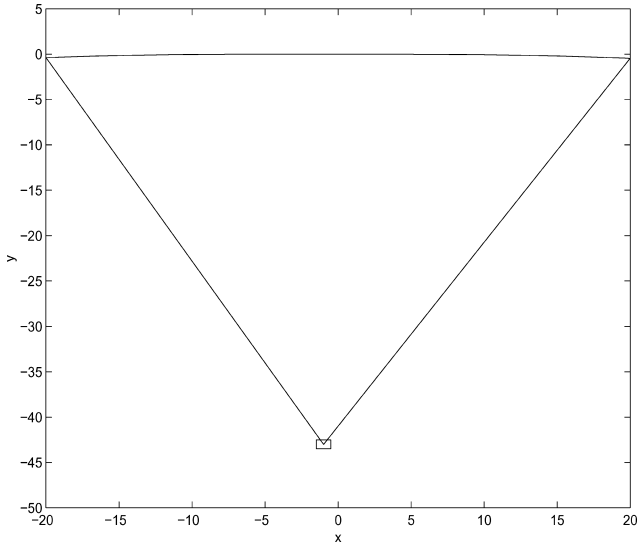


**Fig. 1 Initial state of the rod-cargo system (first simulation). The initial velocity of the cargo is (1, 0) and $\psi(0) = 0$.**

motion. Finally, we couple these effects with a dynamical fluid-structure interaction model using the vortex method.[22–24]

The plan of the paper is as follows: in Sec. II we derive the equations that govern the static model. In Sec. III we introduce the dynamic model. In Sec. IV we present the model for the dynamical fluid-structure interaction. Section V presents the results of some simulations of the model equations. We end up in Sec. VI with some conclusions.

## II. Static Model

To derive a model for the parachute in its static state (with no oscillations or descent), we use the settings shown in Fig. 1. The parachute canopy is modeled by an inextendable flexible and homogeneous rod with linear density $\rho$, moment of inertia (for half the rod) $I$ around 0, and Young's modulus $E$. The cords are assumed to be elastic with elastic constant $k$.

The static system is symmetric around the center line, and hence

$$\boldsymbol{T} = k(h - h_0)\boldsymbol{e} \tag{1}$$

$$m_c g = 2k(h - h_0)\cos\theta \tag{2}$$

The basic equation that governs the rod in its deflected state at equilibrium is[25]

$$\frac{\mathrm{d}\boldsymbol{M}}{\mathrm{d}\ell} = \boldsymbol{F} \times \boldsymbol{t} \tag{3}$$

$$\boldsymbol{F} = -\boldsymbol{T} - \rho g(L/2 - \ell)\boldsymbol{j} \tag{4}$$

$\boldsymbol{M}$ is the moment

$$\boldsymbol{M} = EI\boldsymbol{t} \times \frac{\mathrm{d}\boldsymbol{t}}{\mathrm{d}\ell} \tag{5}$$

For pure bending we have $\boldsymbol{t} = \mathrm{d}\boldsymbol{r}/\mathrm{d}\ell$, $\boldsymbol{r} = (x, y)$, and Eqs. (4) and (5) lead to

$$\frac{\mathrm{d}\boldsymbol{r}}{\mathrm{d}\ell} \times \left( EI\frac{\mathrm{d}^3\boldsymbol{r}}{\mathrm{d}\ell^3} + \boldsymbol{F} \right) = 0 \tag{6}$$

Thus,

$$EI\frac{\mathrm{d}^3\boldsymbol{r}}{\mathrm{d}\ell^3} + \boldsymbol{F} = 0 \tag{7}$$

unless $\mathrm{d}\boldsymbol{r}/\mathrm{d}t$ is parallel to the left-hand side of Eq. (7).

Observe that Eq. (7) has to be solved subject to the constraints of Eqs. (1) and (2) because $\theta$ depends (implicitly) on the deformation of the rod.

If we neglect the mass of the canopy and define $\phi$ as the angle between the tangent to the rod and the $y$ axis then,

$$\frac{\mathrm{d}x}{\mathrm{d}\ell} = \sin\phi, \qquad \frac{\mathrm{d}y}{\mathrm{d}\ell} = \cos\phi \tag{8}$$

and Eqs. (3) and (5) lead to

$$EI\frac{\mathrm{d}^2\phi}{\mathrm{d}\ell^2} = T\sin(\theta - \phi), \qquad T = |\boldsymbol{T}| \tag{9}$$

To determine $\theta$ (approximately), we use Eqs. (1) and (2) and the approximate relation

$$h\sin\theta \cong L/2 \tag{10}$$

which leads to the following fourth-order equation for $\cos\theta$:

$$(L\cos\theta - mg/2k)^2 = 4h_0\cos^2\theta(1 - \cos^2\theta) \tag{11}$$

## III. Dynamical Model

A typical configuration of the rod-cargo system out of equilibrium (but attached without friction to the center point) is shown in Fig. 1. In this configuration two types of dynamical effects have to be taken into consideration. These are as follows: 1, motion of the cargo and oscillations of the rod around 0; and 2, deformations is the shape of the rod caused by dynamical changes in its loading.

Using Fig. 1, we see that is the position of the cargo is $(x, y)$ then its motion is governed by

$$m_c\ddot{x} = T_1\sin\theta_1 - T_2\sin\theta_2 \tag{12}$$

$$m_c\ddot{y} = T_1\cos\theta_1 + T_2\cos\theta_2 - mg \tag{13}$$

where

$$\boldsymbol{T}_1 = k(h_1 - h_0)\boldsymbol{e}_1, \qquad \boldsymbol{T}_2 = k(h_2 - h_0)\boldsymbol{e}_2 \tag{14}$$

and $\boldsymbol{e}_1, \boldsymbol{e}_2$ are unit vectors along the cords.

The oscillations of the rod around its center are caused by the torque exerted by $\boldsymbol{T}_1, \boldsymbol{T}_2$ at the endpoints of the rod. Hence,

$$I(t)\frac{\mathrm{d}^2\psi}{\mathrm{d}t^2} = (\boldsymbol{T}_1 \times \boldsymbol{r}_1 - \boldsymbol{T}_2 \times \boldsymbol{r}_2)\cdot\boldsymbol{k} \tag{15}$$

where

$$I(t) = \rho\int x^2(t)\,\mathrm{d}\ell \tag{16}$$

is changing in time as a result of changes in the shape of the rod.

To determine the (dynamical) shape of the rod, we shall assume that at each moment the force configuration acting on it is quasi-static (that is the rate of change in shape is small). Consequently we can use Eq. (7) to determine the shape of the rod at each moment.

Finally to model the system descent without a full blown modeling of the fluid-structure interaction, one can treat the parachute-cargo system as one body subject to gravity and drag force $D$ (Ref. 8). This leads to

$$\frac{\mathrm{d}(mv_p)}{\mathrm{d}t} = -m_0 g + D, \qquad D = \rho C_D A_h u_p^2/2 \tag{17}$$

In the equations $C_D$ is the lumped (and averaged) value of the drag coefficient that remains unchanged in spite of the dynamical changes in parachute shape.

## IV. Model with Dynamical Fluid-Structure Interaction

To incorporate the fluid-structure (FS) interaction dynamically in our model, one has to simulate the flowfield around the canopy at each time step (talking into account the appropriate shape deformation). In this context the use of a simulation program based on finite elements (or similar) is prohibitive as it requires a new mesh and interpolation of the flow to the new mesh at each time step. This interpolated flow is used then as an initial guess for the transient flow around the new parachute shape. All of this leads to inaccuracies and requires very estensive resources.[26]

To bypass this "bottlenck," we propose using the discrete vortex method to model the FS interaction in the system.

The vortex method has a long history.[27] (This paper gives a general overview of the method and contains an extensive list of references). The application of this method to the parachute system and the FS interaction was carried by the present author[2,3,28] and others.[22,24,29]

In this method the incompressible Navier–Stokes equations

$$\nabla \cdot \boldsymbol{u} = 0, \qquad \boldsymbol{u} = (u, v, w) \tag{18}$$

$$\frac{\partial \boldsymbol{u}}{\partial t} + (\boldsymbol{u} \cdot \nabla)\boldsymbol{u} = -\nabla p + \nu \nabla^2 \boldsymbol{u} \tag{19}$$

are rewritten for the flow vorticity $\boldsymbol{\omega} = \nabla \times \boldsymbol{u}$, which lends to

$$\frac{\partial \boldsymbol{\omega}}{\partial t} + (\boldsymbol{u} \cdot \nabla)\boldsymbol{\omega} = \boldsymbol{\omega} \cdot \nabla \boldsymbol{u} + \nu \nabla^2 \boldsymbol{\omega} \tag{20}$$

In two dimensions $\boldsymbol{\omega} = \omega \boldsymbol{k}$ and $\boldsymbol{\omega} \cdot \nabla \boldsymbol{u} = 0$. Equation (20) reduces to

$$\frac{\partial \boldsymbol{\omega}}{\partial t} + (\boldsymbol{u} \cdot \nabla)\boldsymbol{\omega} = \nu \nabla^2 \boldsymbol{\omega} \tag{21}$$

The essence of the vortex method[22–24] is the discretization of $\omega$ as

$$w(\boldsymbol{x}) = \sum \Gamma_i \delta_\sigma (\boldsymbol{x} - \boldsymbol{x}_i) \tag{22}$$

where $\delta_\sigma$ are (blob) functions approximating the Dirac $\delta$ function, and $\boldsymbol{x}_i$ its position.

The evolution of the invisid flow is given by

$$\frac{\mathrm{d}T_i}{\mathrm{d}t} = 0, \qquad \frac{\mathrm{d}\boldsymbol{x}_i}{\mathrm{d}t} = \boldsymbol{u}(\boldsymbol{x}_i, t) \tag{23}$$

where

$$\boldsymbol{u}(\boldsymbol{x}) = \frac{1}{2\pi} \boldsymbol{e}_z \times \int \frac{(\boldsymbol{x} - \boldsymbol{x}')\omega(\boldsymbol{x})\,\mathrm{d}\boldsymbol{x}'}{|\boldsymbol{x} - \boldsymbol{x}'|^2} \tag{24}$$

The advantage of this method is that it does not require a mesh except for a "circle of vortex creation points" around the solid body in the flow.[23] Furthermore, the discrete vortices aggregate naturally to those regions in the computational domain where the flow gradients are strong and hence provide better flow resolution in these regions.

The net force exerted by the flow on a body is given by[24,29]

$$\boldsymbol{F} = -\rho \frac{\partial}{\partial t} \int_s \boldsymbol{r} \times \boldsymbol{\omega}\,\mathrm{d}s \tag{25}$$

where $\mathrm{d}s$ is an area element. Van der Veget[24] reviews the calculation of the force using the vortex method.

To carry the two-dimensional flow simulation for the parachute system, we used the KDP12 code, which was developed by Spalart.[23] In these simulations the rod represents a two-dimensional cross section of the parachute canopy. For this dynamical, shape-changing geometry, we computed (at each time step) the two-dimensional flow around the rod. The KDP12 code calculates also the drag and lift coefficients as well as the pitching moment on the rod. This enables us to compute a dynamical value for these coefficients at each time step and incorporate these in the simulation of the parachute-cargo system. We observe however that this code does not take into account the possible change in $C_D$ caused by flexible boundaries.[10,28,30,31] Accordingly, out current simulation ignores the effects of flutter on the canopy and treats it as a bluff body.

The modified equations for parachute oscillations and descent become

$$I(t)\frac{\mathrm{d}^2\psi}{\mathrm{d}t^2} = (\boldsymbol{T}_1 \times \boldsymbol{r}_1 - \boldsymbol{T}_2 \times \boldsymbol{r}_2) \cdot \boldsymbol{k} + \boldsymbol{M}_{\mathrm{fs}} \tag{26}$$

$$\frac{\mathrm{d}(mu_p)}{\mathrm{d}t} = F_L \tag{27}$$

$$\frac{\mathrm{d}(mv_p)}{\mathrm{d}t} = -m_0 g + D(t) \tag{28}$$

where $F_L = \rho C_L A_v u^2/2$. Furthermore, the resultant stress on a cross section of the rod is modified to be

$$\boldsymbol{F} = -\boldsymbol{T} - \rho g(L/2 - \ell)\boldsymbol{j} + p\boldsymbol{n} \tag{29}$$

## V. Simulation Methodology and Results

The simulation of the parachute-cargo system with the FS interaction proceeded as follows.

At first we computed an initial shape of the system based on the initial conditions but without the FS interaction. Using this shape, we iterated the KDP12 code to obtain an initial flowfield, which was represented by 6000 vortices. Equations (29) and (7) were then used to obtain a new initial shape for the parachute.

With this shape and initial conditions we used Eqs. (12), (13) and (26–28) to obtain the new position of the cargo, the pitching angle $\psi$, and $\boldsymbol{u}_p$ at time $\Delta t$. This information was used to compute (iteratively) the new parachute shape. The flowfield around this new shape was computed then using 100 iterative steps in the vortex simulation program, and the process was repeated. These three major parts of the computation were performed at each time step whose size varied according to the stiffness of the problem.

For the first part of the computation, a sixth-order Runge–Kutta integrator was used with relative error of $10^{-4}$. The second part required an iterative procedure. In each iteration we computed first a new shape based on Eq. (7) using the same Runge–Kutta just mentioned with same error. This shape gave rise to a change in the cords tension, and with this new tension a new shape was computed. The iterations continued until the relative change in the tension and shape were less than $10^{-4}$. In other parts of the program (e.g., computation of the parachute volume), an absolute error limit of $10^{-4}$ was maintained. As to the computation of the drag coefficient, one should bear in mind that the vortex method is statistical in nature. One can compute (a posteriori) the averaged standard deviation in the values of the drag coefficient (taking into account the last 50 iterations at each time step). With the 6000 vortices that were used in the simulation, we found this averaged standard deviation to be of the order of 0.1.

In the following we present the results of two simulations using the model presented in the preceding sections. In the first simulation the parachute and cargo are almost vertical in their initial state. The second simulation represents a more realistic initial state in which both parachute and cargo are "far" from the vertical state. (In both simulations $\boldsymbol{u}_p = 0$ at $t = 0$).

The parameters used in these simulations are as follows (parameters for the second simulation, which are different from the first, are in parentheses): $E = 1000$ Newton/kg, $L = 40$ m, $h_0 = 40$ m, $k = 200$ Newton/m, $m_c = 1000\,(6000)$ kg, $\rho = 1.8$ kg/m, $\rho_A = 1.27$ kg/m$^3$, and $\nu = 1.8 * 10^{-5}$ m$^2$/s. The initial conditions on the cargo and $\psi$ in these simulations were as follows:

$$\boldsymbol{x}_c = (0, -43), \qquad ((2, -44)), \qquad \boldsymbol{v}_c = (1, 0)$$

$$((0, 0)), \qquad \text{and} \qquad \psi = 0(\pi/18)$$

Some of the results of these simulations are presented in Figs. 1–12.

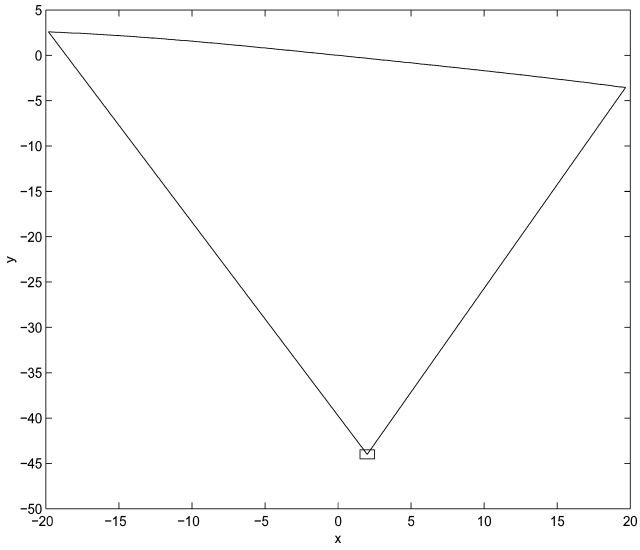


**Fig. 2 Initial state of the rod-cargo system (second simulation). The initial velocity of the cargo is (0, a0) and $\psi(0) = \pi/18$.**

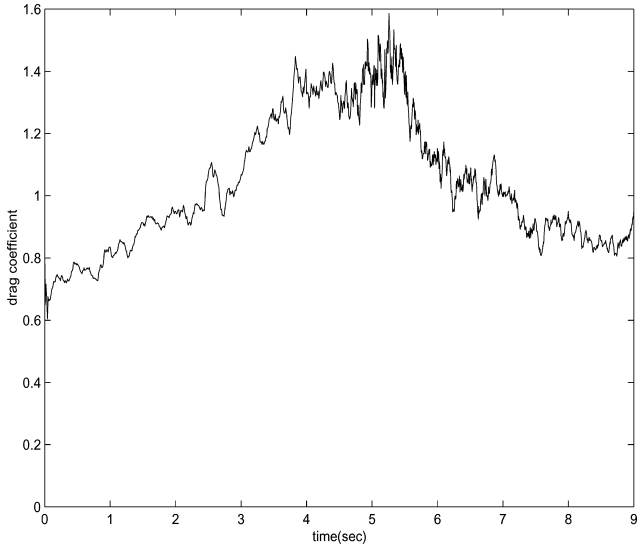


**Fig. 3 Value of the drag coefficient as a function of time for the first simulation.**

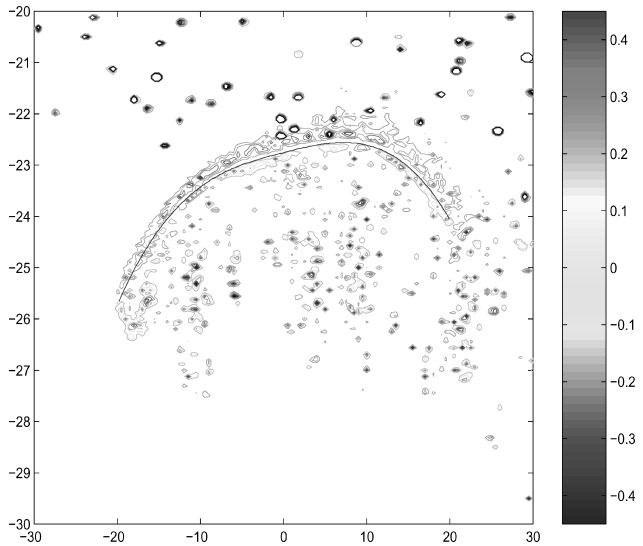

**Fig. 4 Vorticity field around the parachute at time 5.08 s. First simulation.**

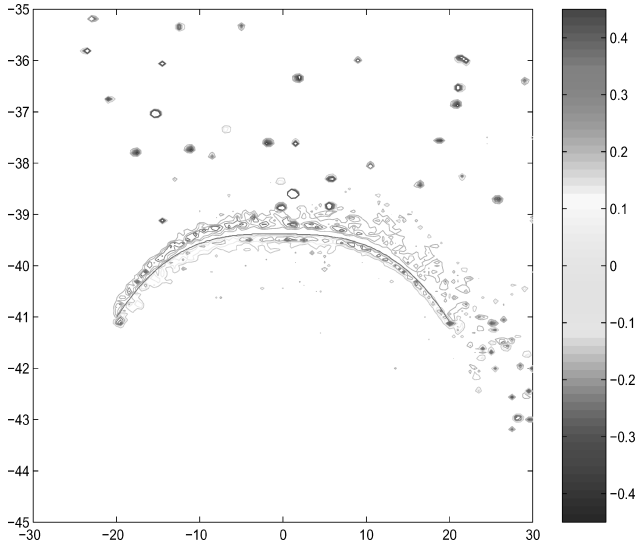

**Fig. 5 Vorticity field around the parachute at time 7.58 s. First simulation.**

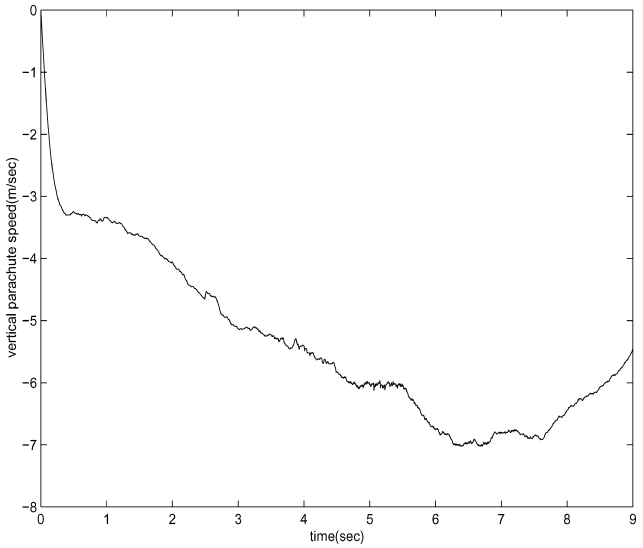


**Fig. 6 Parachute vertical velocity. First simulation.**

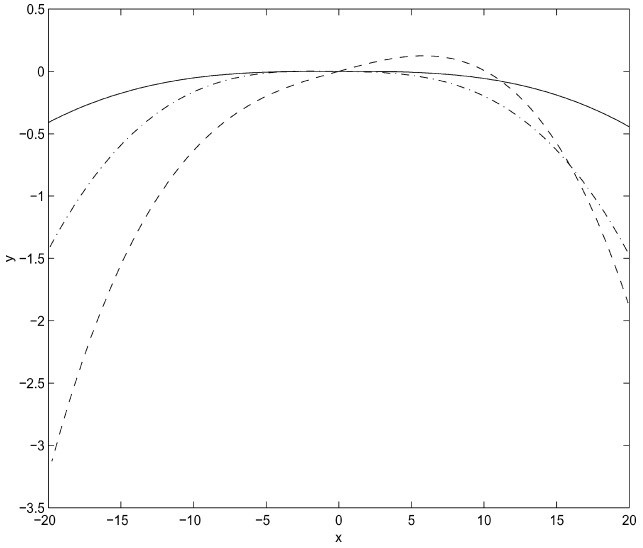


**Fig. 7 Rod shape at times 0 s (——), 2.7 s (– · – · –), and 5 s (– – –). First simulation.**

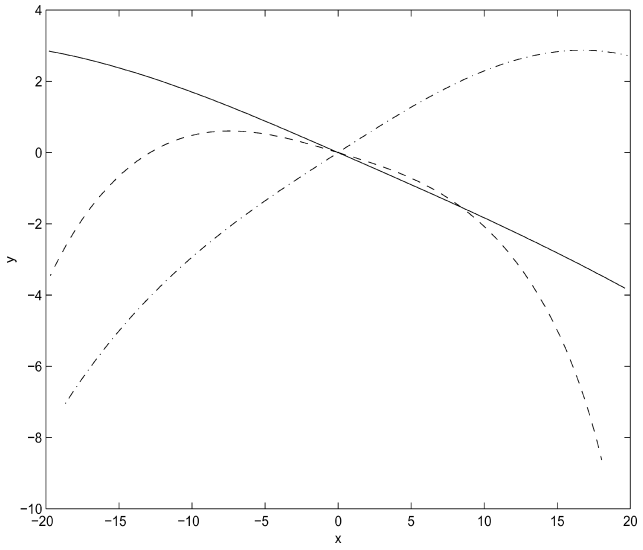


**Fig. 8 Rod shape at times 0 s (——), 2.7 s (– · – · –), and 5 s (– – –). Second simulation.**

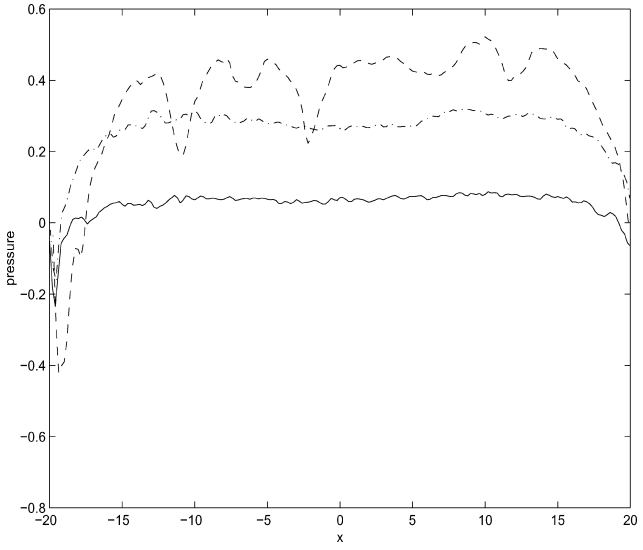


**Fig. 9 Fluid pressure on the parachute canopy caused by the fluid-structure interaction. First simulation and same times as Fig. 4.**

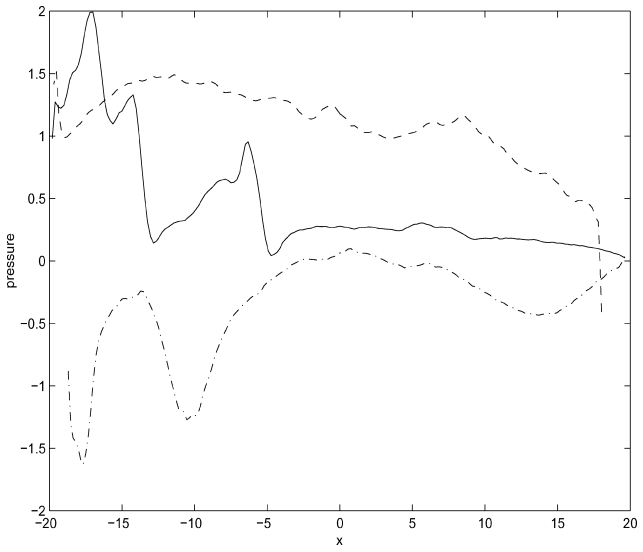


**Fig. 10 Fluid pressure on the parachute canopy caused by the fluid-structure interaction. Second simulation and same times as Fig. 5.**

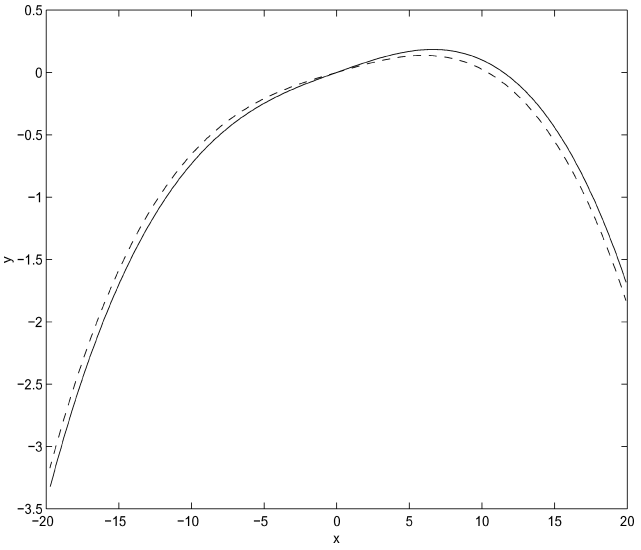


**Fig. 11 Shape of the rod with (– – –) and without (——) fluid-structure interaction. First simulation at time 5.1 s.**

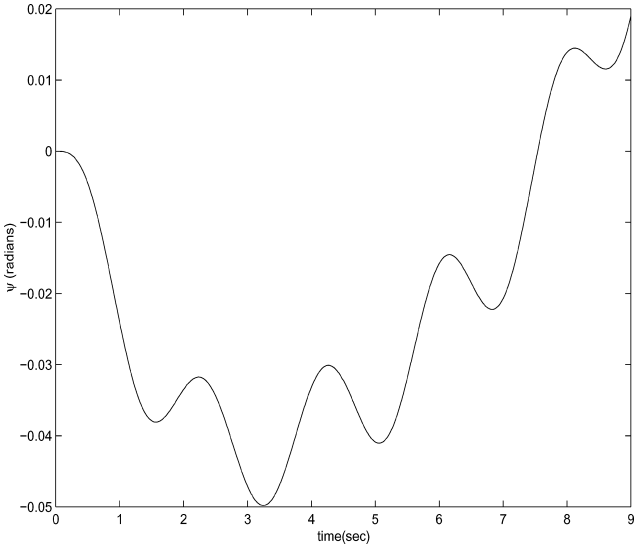


**Fig. 12 Parachute pitching angle as a function of time. First simulation.**

Figures 1 and 2 depict the initial state of the system for the two simulations. Figure 3 shows the dynamical value of the drag coefficient in the first simulation as a function of time. The drag coefficient in this figure is "noisy" because of the statistical nature of the vortex method. We observe that the peak in the value of this coefficient is caused by vortex shading and variations in canopy shape. These are demonstrated in Figs. 4 and 5, which compare the vorticity field near the parachute at time $t = 5.08$ s (near the peak in the value of the drag) and $t = 7.58$ s. In Fig. 6 we plot the vertical parachute velocity vs time. Initialy this velocity increases because $\boldsymbol{u}_p = 0$ at $t = 0$. Around $t = 5$ s it flattens out because of the increase in $C_D$ and then increases again as $C_D$ decreases.

Figures 7–10 represent respectively the shape and fluid pressure (caused by the FS interaction) at three different times during these simulations. Figure 11 compares the parachute shape with and without the FS interaction at $t = 4$ s for the first simulation. (The simulation without the FS interaction used the initial conditions of the first simulation with constant value for $C_D = 1.5$ – as in Ref. 8). Finally Fig. 12 shows the oscillation in the pitching angle of the parachute as a function of time. One can see clearly the damping of these oscillations as the parachute and the cargo "attempt" to align in the vertical direction. The increase in the pitching angle during the first cycle is caused by the initial position

of cargo relative to the parachute and the length of the cords. This figure does not yield a direct relation between these oscillations and parachute deformations, which are not easy to quantify. However we note that the system starts to align itself vertically at around $t = 4$ s, and this is exactly when the drag coefficient (which by itself depends on these deformations) has increased to about 1–1.2

These simulations demonstrate that even the initial model presented in this paper is able to reproduce correctly some key elements of parachute dynamical behavior after deployment and hence provide some new insights about this dynamics.

## VI. Conclusions

The dynamical model presented in this paper has a finite number of degrees of freedom. As such, it is a projection of the complete system dynamics on a finite dimensional space. In any such projection one can only hope to capture the main features of the dynamical system under consideration. Such models are important as they can provide insights that are hard to come by from numerical studies (or models that incorporate many degrees of freedom). In particular the present model might prove to be valuable when one attempts to study problems related to parachute collapse and failure. To this end, one must perform a bifurcation analysis of the dynamical equations derived in this paper and the qualitative structure of its solutions as a function of the various parameters and initial conditions.

The most important step towards the refinement of the present model will be to replace the (one) rod representing the canopy by a flexible plate (or membrane) or several rods in three-dimensional configuration. In addition a refined three-dimensional model for the fluid-structure interaction in this system is needed.

The bifurcations of the model equations in two-dimensions and a study of the three-dimensional model just referred to are currently under study by the present author.

## References

[1]Steeves, E. C., "Analysis of Decelerators in Motion Using Computational Fluid Dynamics," *Proceedings of the AIAA 10th Aerodynamics Decelerator System Technology Conference*, AIAA, Washington, DC, 1989, pp. 86–90; also AIAA Papers 89/876-89/944.

[2]Humi, M., "Drag Computation by Vortex Methods," *Journal of Aircraft*, Vol. 29, No. 5, 1992, pp. 819–822.

[3]Humi, M., "Turbulent Effects on Parachute Drag," *Journal of Aircraft*, Vol. 32, No. 3, 1995, pp. 682–684.

[4]Johari, H., and Desabrais, K. J., "Scaling for Solid Cloth Parachutes," AIAA Paper 2001-2007, May 2001.

[5]Balligand, H., and Higuchi, H., "Experimental Investigation of the Wake Behind a Solid Disk," Sandia Rept. SAND-90-7083, Sandia National Lab., Albuquerque, NM, Dec. 1993, p. 166.

[6]Ross, E. W., Jr., "Approximate Analysis of a Flat Circular Parachute in Steady Descent," *Journal of Aircraft*, Vol. 7, No. 3, 1970, pp. 266–271.

[7]Ross, E. W., Jr., "A Nonlinear Solution for Parachute Suspension Line Deformation," *Journal of Aircraft*, Vol. 22, No. 10, 1985, pp. 925, 926.

[8]Ross, E. W., Jr., "A General Theory of Parachute Opening," *Journal of Aircraft*, Vol. 9, No. 4, 1972, pp. 257, 258.

[9]Piscitelle, L. J., "Dynamical System Analysis of an Aerodynamic Decelerator: Bifurcation to Divergence and Flutter," *Future Directions of Nonlinear Dynamics in Physical and Biological Systems*, edited by P. L. Christainsen, J. C. Eilbeck, and R. D. Parmentier, Plenum, New York, 1993, pp. 161–164.

[10]Strickland, J. H., "Axisymmetric Bluff-Body Flow: A Vortex Solver for Thin Shells," Sandia Rept. SAND-91-2760, Sandia National Lab., Albuquerque, NM, May 1992, p. 67.

[11]Wolf, D. E., "A Simplified Dynamic Model of Parachute Inflation," *Journal of Aircraft*, Vol. 11, No. 1, 1974, pp. 28–33.

[12]McVey, D. F., and Wolf, D. E., "Analysis of Deployment and Inflation of Large Ribbon Parachutes," *Journal of Aircraft*, Vol. 11, No. 1, 1974, pp. 96–103.

[13]Macha, J. M., "A Simple Approximate Model of Parachute Inflation," AIAA Paper 93-1206, May 1993.

[14]Doherr, K. F., and Saliaris, C., "On the Influence of Stochasitc and Acceleration Dependent Aerodynamic Forces on the Dynamic Stability of Parachutes," AIAA Paper 81-1941, Oct. 1981.

[15]Eaton, J. A., "Added Mass and the Dynamic Stability of Parachutes," *Journal of Aricraft*, Vol. 19, No. 5, 1982, pp. 414–416.

[16]White, F. M., and Wolf, D. F., "A Theory of Three-Dimensional Parachute Dynamic Stability," *Journal of Aircraft*, Vol. 5, No. 1, 1968, pp. 86–92.

[17]Doherr, K. F., "Theoretical and Experimental Investigation of Parachute-Load-System Dynamic Stability," AIAA Paper 75-1397, 1975.

[18]Tory, C., and Ayres, R., "Computer Model of a Fully Deployed Parachute," *Journal of Aircraft*, Vol. 14, No. 7, 1977, pp. 675–679.

[19]Eaton, J. A., and Cockrell, D. J., "The Validity of the Leicester Computer Model for a Parachute with Fully-Deployed Canopy," AIAA Paper 79-0460, 1979.

[20]Yavuz, T., and Cockrell, D. J., "Experimental Determination of Parachute Apparent Mass and Its Significance in Predicting Dynamic Stability," AIAA Paper 81-1920, 1981.

[21]Cockrell, D. J., and Doherr, K. F., "Preliminary Cosiderations of Parameter Identification Analysis from Parachute Aerodynamic Flight Test Data," AIAA Paper 81-1940, 1981.

[22]Blevins, R. D., "Application of the Discrete Vortex Method to Fluid-Structure Interaction," *Journal of Pressure Vessel Technology*, Vol. 113, No. 3, 1991, pp. 437–445.

[23]Spalart, P. R., "Vortex Methods of Separated Flows," NASA TM 100068, June 1988, p. 66.

[24]Van der Veget, J. J., "Calculation of Forces and Moments in Vortex Methods," *Journal of Engineering Mathematics*, Vol. 22, No. 3, 1988, pp. 225–238.

[25]Landau, L. D., and Lifshitz, E. M., *Theory of Elasticity*, 3rd ed., Pergamon, New York, 1993, Chap. 2.

[26]Stein, K. R., Benney, R. J., Tezduyar, T. E., Leonard, J. W., and Accorsi, M. L., "Fluid Structure Interactions of a Round Parachute," *Journal of Aircraft*, Vol. 38, No. 5, 2001, pp. 800–808.

[27]Leonard, A., "Computing Three Dimensional Incompressible Flow with Vortex Methods," *Annual Review of Fluid Mechanics*, Vol. 17, 1985, pp. 523–564.

[28]Humi, M., "Three Dimensional Vortex Method for Parachutes," *International Journal for Numerical Methods in Fluids*, Vol. 16, No. 10, 1993, pp. 879–890.

[29]Wu, J. C., "Theory of Aerodynamic Force and Moment in Viscous Flow," *AIAA Journal*, Vol. 19, No. 4, 1981, pp. 432–441.

[30]Benjamin, T. B., "Fluid Flow with Flexible Boundaries," *Proceedings of the 11th International Congress in Applied Mechanics*, edited by H. Gortler, Springer-Verlag, Berlin, 1966, pp. 109–126.

[31]Cottet, G.-H., and Koumoutsakos, P. D., *Vortex Methods Theory and Practice*, Cambridege Univ. Press, Cambridge, England, UK, 2000.